SplitFed: When Federated Learning Meets Split Learning

Preprint · April 2020

CITATIONS
0

READS
686

3 authors:

Chandra Thapa
The Commonwealth Scientific and Industrial Research Organisation
23 PUBLICATIONS **135** CITATIONS
SEE PROFILE

M.A.P. Chamikara
RMIT University
56 PUBLICATIONS **167** CITATIONS
SEE PROFILE

Seyit A Camtepe
The Commonwealth Scientific and Industrial Research Organisation
81 PUBLICATIONS **3,183** CITATIONS
SEE PROFILE

SplitFed: When Federated Learning Meets Split Learning

Chandra Thapa[1], M.A.P. Chamikara[1,2], and Seyit Camtepe[1]

[1] CSIRO Data61, Australia
[2] RMIT University, Australia
{chandra.thapa, chamikara.arachchige, seyit.camtepe}@data61.csiro.au
pathumchamikara.mahawagaarachchige@rmit.edu.au

Abstract. Federated learning (FL) and split learning (SL) are two recent distributed machine learning (ML) approaches that have gained attention due to their inherent privacy-preserving capabilities. Both approaches follow a model-to-data scenario, in that an ML model is sent to clients for network training and testing. However, FL and SL show contrasting strengths and weaknesses. For example, while FL performs faster than SL due to its parallel client-side model generation strategy, SL provides better privacy than FL due to the split of the ML model architecture between clients and the server. In contrast to FL, SL enables ML training with clients having low computing resources as the client trains only the first few layers of the split ML network model. In this paper, we present a novel approach, named splitfed (SFL), that amalgamates the two approaches eliminating their inherent drawbacks. SFL splits the network architecture between the clients and server as in SL to provide a higher level of privacy than FL. Moreover, it offers better efficiency than SL by incorporating the parallel ML model update paradigm of FL. Our empirical results considering uniformly distributed horizontally partitioned datasets and multiple clients show that SFL provides similar communication efficiency and test accuracies as SL, while significantly reducing - around five times - its computation time per global epoch. Furthermore, as in SL, its communication efficiency over FL improves with the increase in the number of clients.

1 Introduction

Machine learning (ML) usually relies on large datasets and high computational resources. For example, deep learning (DL) is a type of ML that requires extensive computing resources (e.g., GPUs) as well as large datasets to produce high accuracy [1,2]. Due to the excellent learning capabilities, DL is heavily used in several fields, including healthcare and finance, which often operate on privacy-sensitive data. Moreover, data are usually distributed and isolated in these fields due to privacy concerns. For example, in a healthcare system, data reside in hospitals, imaging centers, and research centers that are located in different locations.

For ML, a straightforward approach is to conduct a central pooling of the raw data. Then, analysts access the central repository of the pooled data to conduct ML over the overall dataset. This approach is called Data-to-Modeler (DTM) [3]. However, it has challenges due to ethical requirements, regulation (e.g., GDPR in Europe [4]), privacy concern, single-point failure, competitiveness between the data custodians, and scalability issues.

The second approach is to leverage distributed collaborative learning (DCL). It enables computation on multiple systems or servers and end devices such as mobile phones, while data reside in the source devices. As the distributed data are not pooled to one central repository, DCL provides a level of privacy to the datasets. However, there can still be privacy risks as the server or distributed systems may not be trusted platforms. In this regard, various techniques, including homomorphic encryption (HE) [5], differential privacy (DP) [6], multi-party computation (MPC) [7], and distributed collaborative machine learning (DCML) have been proposed for privacy-preserving computations. These techniques enable privacy-by-design in the system. HE and MPC are cryptographic approaches and face challenges, including high computational requirements, communication cost, and the necessity of participants being online all time. Low efficiency in ML model training and high communication latency are two main drawbacks of the existing DP approaches. In DCML, the analyst has no access to the raw data; instead, ML model is submitted to the data curator for processing. This approach is called Model-to-data (MTD) [3] and depicted in Fig. 1. It enables data processing without accessing the raw data. This way, MTD provides privacy to sensitive raw data. On the top of this, DCML can integrate DP or HE [8] and MPC [9] to provide robust privacy.

Federated learning (FL) [10,11], split learning (SL) [12], and distributed synchronous SGD [13] are the most popular DCML approaches. Although DCML optimization has been a frequently addressed topic, in this work, our primary focus is on privacy preservation and efficiency in DCML. In this regard, based on whether the machine learning model is split and trained separately or not, we broadly divide these approaches into two types; the first type is without network splitting, e.g., FL and distributed synchronous SGD, and the second type with network splitting, e.g., SL. Distributed synchronous SGD (e.g., downpour SGD [14]) works in a similar essence to FL. The difference

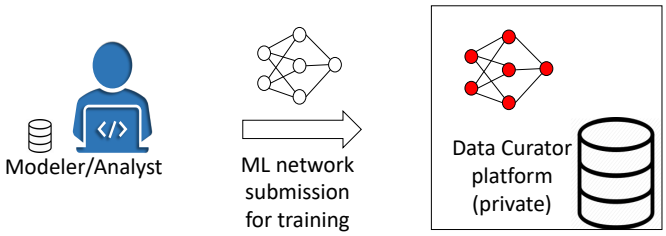

Fig. 1: Model-to-data approach

is that the (local and global) updates are based on one batch of training data in the distributed synchronous SGD, whereas, in FL, a client trains the network over its all local data for some time, i.e., local epochs[3], before updating the model to the server. Considering the similarity and high latency in distributed synchronous SGD, we choose only FL from the first type in this work.

The main advantage of FL is that it allows parallel (hence efficient) ML model training across multiple clients, whereas the main advantage of SL is that it provides better privacy due to the split of the ML model between the clients and the server. This offers two benefits. Firstly, the model privacy as the client has no access to the server-side model and vice-versa. Secondly, assigning only a part of the network to train at the client-side reduces processing load (compared to that of running the complete network), which is significant in ML computation on resource constrained devices. However, due to the sequential nature of ML model training across the clients, SL is significantly slower than FL. Now by considering the pros and cons of FL and SL, we have a natural question: *Can we combine the SL and FL in some sense to exploit their main advantages?*

As an answer, we propose a novel architecture that integrates FL and SL together to produce *splitfed learning (SFL)* (Section 2.3). SFL provides an excellent solution that offers better privacy than FL, and it is faster than SL with a similar performance in the model accuracy and communication efficiency (Section 6). Moreover, SFL enables distributed processing across clients with low computing resources as SL, but with an improvement in its training speed, which is around five times based on empirical studies (Section 6.4). Thus, it is beneficial for ML-based real-time analysis in time-critical applications in various domains, including health, e.g., real-time anomaly detection in network with multiple medical internet of things[4] connected via gateways, and finance, e.g., privacy-preserving credit card fraud detection.

2 Background

2.1 Federated Learning

Federated learning [10,11,15] is a collaborative machine learning technique developed by google to train machine learning algorithms on distributed devices, including mobile phones. It pushes the computations to the edge devices and removes the necessity to pool the raw data out from the data curator for training an ML algorithm. This way, it enables the privacy of the raw data. In FL, a complete ML network/algorithm is trained by each client on its local data in parallel for some local epochs, and then they send the local updates to the server. Afterward, the server aggregates the local updates from all clients and form a global model by federated averaging. The global model is then sent back to all clients to train for the next round. This process continues until the algorithm converges to a certain level. For more detail, refer to Algorithm 1 (which is also known as FederatedAveraging algorithm).

2.2 Split Learning

Split learning [16,12,17] is a collaborative deep learning technique, where a deep learning network $\mathbf{W}$ is split into two portions $\mathbf{W}^{\mathrm{C}}$ and $\mathbf{W}^{\mathrm{S}}$, called client-side network and server-side network, respectively. $\mathbf{W}$ includes weights, bias, and hyperparameters. The clients, where the data reside, commit only to the client-side portion of the network, and the server commits only to the server-side portion of the network. The client-side and server-side portions collectively

[3] In one local epoch of a client, there is a completion of one forward and its respective back-propagation for all available local data at that client.

[4] Examples of medical internet of things (MIoTs) include a glucose monitoring device, an open artificial pancreas system, a wearable electrocardiogram (ECG) monitoring device, and a smart lens.

Table 1: Notations

t	Round (time instance)	$\nabla\ell$	Gradient of the loss ℓ
k, K	K clients, each indexed by $k \in \{1, 2, \ldots, K\}$	η	Learning rate
$\mathbf{W}$	Joint global machine learning model	E	No. of local epochs at client side
$\mathbf{W}_t$	$\mathbf{W}$ at t	$\mathcal{B}$	A set of batches of local data
$\mathbf{W}^{\text{C}}_{k,t}$	Client-side model of client k at t	S_t	A set of n_t clients at t, $n_t \leq K$
$\mathbf{W}^{\text{S}}_t$	Server-side Model at t	$\mathbf{A}_t$	All activations at t
$f(x; y)$	Any function f on input x given y	$\mathbf{A}_{k,t}$	Activations of the cut layer (i.e., smashed data) of client k at t
$\mathbf{Y}_k$	True labels from the client k	$\hat{\mathbf{Y}}_k$	Predicted labels for the client k

Algorithm 1: Federated learning [11]. Model $\mathbf{W}$ is a global model, and the fraction of the participant C is kept 1 (i.e., $n_t = K$).

```
/* Runs on Server */
Ensure the Server executes at round t ≥ 0:
    Distribute W_t to a random subset S_t of K clients
    for each client k ∈ S_t in parallel do
        W_{k,t} ← ClientUpdate(W_{k,t})          ▷ Receives updates from n_t clients
    end
    Perform W_{t+1} ← Σ_{k=1}^{K} (n_k/n) W_{k,t}   ▷ n = Σ_k n_k, and server performs weighted average of the gradients and update the model
/* Runs on Client k */
EnsureClientUpdate(W_{k,t}):
    Set W_{k,t} = W_t                            ▷ W_t is downloaded from server
    for each local epoch e from 1 to E do
        for batch b ∈ B do
            Forward (calculate loss), back-propagation (calculate ∇ℓ(W_{k,b,t}))
            W_{k,t} ← W_{k,t} − η∇ℓ(W_{k,b,t})
        end
    end
    Send W_{k,t} to server                       ▷ n_k is the entire size of the dataset at each client
```

form the full network $\mathbf{W}$. The training of the network is done by a sequence of a distributed training processes. In a simple setup, the forward propagation and the back-propagation take place in the following way: With the raw data, a client trains the network up to a certain layer of the network, called the *cut layer*, and sends the activations of the cut layer, also called *smashed data*, to the server. Then, the server carries out the training of the remaining layers with the smashed data that it received from the client. This completes a single forward propagation. Next, the server carries out the back-propagation up to the cut layer and sends the gradients of the smashed data to the client. With the gradients, the client carries out its back-propagation on the remaining network (i.e., up to the first layer of the network). This completes a single pass of the back-propagation between a client and the server. This process of forward propagation and back-propagation continues until the network gets trained with all the available clients and reaches its convergence. In SL, the architectural configurations are assumed to be conducted by a trusted party who has direct access to the main server. This authorized party selects the ML model (based on the application) and network splitting (finding the cut layer) at the beginning of the learning. The synchronization of the learning process with multiple clients is done either in centralized mode or peer-to-peer mode. In the centralized mode, before starting training with the (main) server, a client updates its client-side model by downloading it from a trusted third-party server, which retains the updated client-side model uploaded by the last trained client. On the other hand, in peer-to-peer mode, the client updates its client-side model by directly downloading it from the last trained client. Overall, the training takes place in a relay-based approach, where the server trains with one client and then move to another client sequentially. The SL algorithm is provided in Algorithm 2.

SL limits the client-side network portion up to a few layers. Thus, it enables the reduction in client-side computation in comparison to other collaborative learning such as FL, where the complete network is trained at the client-side. Besides, in the SL setup, the client-side updates, and the updated model $\mathbf{W}^{\text{C}}$ are not accessible to the server once the training starts. The server knows only the portion of the network it trains, i.e., $\mathbf{W}^{\text{S}}$. Consequently,

Algorithm 2: Split learning with label sharing[16]. The learning rate η remains same in both server and client side.

/* Runs on Server */
EnsureMainServer executes at round $t \geq 0$**:**
  for a request from client $k \in S_t$ with new data **do**
    $(\mathbf{A}_{k,t}, \mathbf{Y}_k) \leftarrow$ ClientUpdate$(\mathbf{W}^{\mathrm{C}}_{k,t})$ ▷ $\mathbf{A}_{k,t}$ *and* $\mathbf{Y}_k$ *are from client* k
    Forward propagation with $\mathbf{A}_{k,t}$ on $\mathbf{W}^{\mathrm{S}}_t$ ▷ $\mathbf{W}^{\mathrm{S}}_t$ *is the server-side part of the model* $\mathbf{W}_t$
    Loss calculation with $\mathbf{Y}_k$ and $\hat{\mathbf{Y}}_k$
    Back-propagation and model updates with learning rate η: $\mathbf{W}^{\mathrm{S}}_{t+1} \leftarrow \mathbf{W}^{\mathrm{S}}_t - \eta \bigtriangledown \ell(\mathbf{W}^{\mathrm{S}}_t; \mathbf{A}^{\mathrm{S}}_t)$
    Send $d\mathbf{A}_{k,t} := \bigtriangledown \ell(\mathbf{A}^{\mathrm{S}}_t; \mathbf{W}^{\mathrm{S}}_t)$ (i.e., gradient of the $\mathbf{A}_{k,t}$) to client k for its ClientBackprop$(d\mathbf{A}_{k,t})$
  end

/* Runs on Client k */
EnsureClientUpdate$(\mathbf{W}^{\mathrm{C}}_{k,t})$**:**
  Set $\mathbf{A}_{k,t} = \phi$
  if Client k is the *first* client to start the training **then**
    $\mathbf{W}^{\mathrm{C}}_{k,t} \leftarrow$ Randomly initialize (using Xavier or Gaussian initializer)
  else
    $\mathbf{W}^{\mathrm{C}}_{k,t} \leftarrow$ ClientBackprop$(d\mathbf{A}_{k-1,t-1})$ ▷ $k-1$ *is the last trained client with the main server*
  end
  for each local epoch e from 1 to E **do**
    for batch $b \in \mathcal{B}$ **do**
      Forward propagation on $\mathbf{W}^{\mathrm{C}}_{k,b,t}$ ▷ $\mathbf{W}^{\mathrm{C}}_{k,t}$ *of batch* b*, where* $\mathbf{W}^{\mathrm{C}}_{k,t}$ *is the client-side part of the model* $\mathbf{W}_t$
      Concatenate the activations of its final layer to $\mathbf{A}_{k,t}$
      Concatenate respective true labels to $\mathbf{Y}_k$
    end
  end
  Send $\mathbf{A}_{k,t}$ and $\mathbf{Y}_k$ to server

/* Runs on Client k */
EnsureClientBackprop$(d\mathbf{A}_{k,t})$**:**
  for batch $b \in \mathcal{B}$ **do**
    Back-propagation with $d\mathbf{A}_{k,b,t}$ ▷ $d\mathbf{A}_{k,t}$ *of the batch* b
    Model updates $\mathbf{W}^{\mathrm{C}}_{t+1} \leftarrow \mathbf{W}^{\mathrm{C}}_t - \eta\ d\mathbf{A}_{k,b,t}$
  end
  Send $\mathbf{W}^{\mathrm{C}}_{t+1}$ to the next client ready to train with the main server.

SL provides a certain level of privacy to both the trained model and the inputs because the server needs to predict all parameters of the client-side network to infer the information. In contrast, the server has full access (i.e., white box access) to the whole trained network in FL. However, there is a primary issue with SL. The relay-based training in SL makes the clients' resources idle because only one client engages with the server at one instance. This significantly increases the training overhead if there are many clients.

2.3 Splitfed Learning

In this section, we present splitfed learning that utilizes the strengths of SL and FL. SFL combines the strength of FL, which is parallel processing among distributed clients, and the strength of SL, which is network splitting (client-side and server-side) during training. Refer to Fig. 2 for the SFL system model. The right-hand side of the figure shows how the clients and the (main) server perform the network training. Unlike SL, all clients (e.g., Hospitals, MIoTs with low computing resources) carry out the forward propagations on their client-side model in parallel, then pass their smashed data to the (main) server. Then the server, which is assumed to have sufficient computing resources (e.g., cloud server and researchers with high-performance computing resources), process the forward propagation and back-propagation on its server-side model with each client's smashed data in (somewhat) parallel. Then, it sends the gradients of the smashed data (i.e., activations' gradients) to the respective clients for their back-propagation. Afterward, the server updates its model by a weighted average of the gradients that it computes during the back-propagation on each client's smashed data. At the client's side, after receiving the gradients of the smashed data, each client performs the back-propagation on their client-side local model and computes its gradients. Then, the clients send the gradients to the fed server, which conducts the federated averaging of the client-side local updates and send back to all participating clients. This way, the fed server synchronizes the client-side global model in each round of network training. The fed server's computations are not costly, and it is hosted within the local

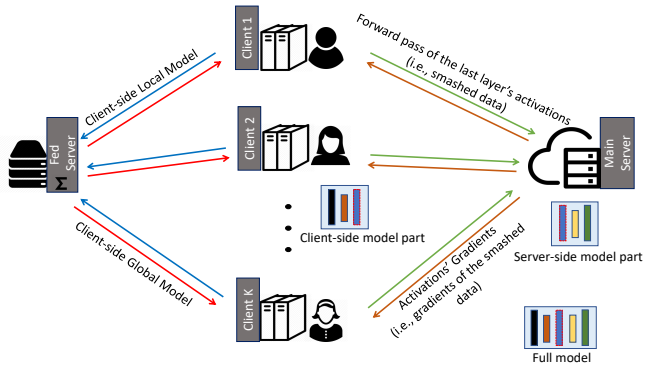

Fig. 2: Splitfed system model

edge boundaries. For more detail, refer to the SFL algorithm in Algorithm 3. Although the algorithm is for the label sharing configuration, all possible configurations of SL, including U-shaped without label sharing, vertically partitioned data, extended vanilla, and multi-task SL [16], can be carried out similarly in SFL.

Table 2: Comparative description of split, federated and splitfed learning

Learning approach	Model aggregation	Privacy advantage by splitted model (client & server sides)	Client-side training	Distributed computing	Access to raw data
Split	No	Yes	Sequential	Yes	No
Federated	Yes	No	Parallel	Yes	No
Splitfed (proposed)	Yes	Yes	Parallel	Yes	No

A brief comparative description of SL, FL, and SFL is provided in Table 2.

Variants of splitfed learning We propose two variants of SFL. The first one is called *splitfedv1 (SFLV1)*, which is depicted in Algorithm 3. We present the next algorithm, called *splitfedv2 (SFLV2)*, motivated from the intuition of possibility to increase the model accuracy by removing the model aggregation part in the server-side computation module in Algorithm 3. In this algorithm, the server-side models of all clients are executed in parallel and aggregated to obtain the global server-side model at each global epoch[5]. In contrast, SFLV2 processes the forward-backward propagations of the server-side model sequentially with respect to the client's smashed data. The model gets updated in every single forward-backward propagation. Besides, the server receives the smashed data from all participating clients at one time in parallel, and the client-side operations remain the same as in the SFLV1.

3 Total cost analysis of federated, split and splitfed learning

Assume that K be the number of clients, p be the total data size, q be the size of the smashed layer, $|W|$ be the total number of model parameters, β be the fraction of model parameters (weights) available in a client in SL, t be the model training time (for any architecture) for one global epoch, and T be the wait time (delay) for one client to receive updates during SL during one global epoch. Table 3 provides the communication costs and the total costs of each of the DCML approaches for one global epoch. The term $K|W|$ in FL training time is due to the latency caused by federated averaging, and the term $2\beta|W|$ in communication per client is due to the download and upload of the client-side model updates before and after training, respectively, by the client. As shown in the table, due to T, SL can become inefficient when there is a large number of clients (refer to Fig. 6 for an empirical result). Besides, we see that when K increases, the total cost (communication and computation) increases in the order of SFLV2<SFLV1<SL, which can also be observed in Fig. 5 and 6.

[5] When forward propagation and back-propagation are completed for all available datasets across all participating clients for one time, then it is called one global epoch.

Algorithm 3: Splitfed learning (our approach) with label sharing. The splitfed network ($\mathbf{W}$) configuration follows the same setup used in SL. Learning rate η remains the same for the server-side model and the client-side model.

/* Runs on Main Server */
EnsureMainServer executes at round $t \geq 0$**:**
  for each client $k \in S_t$ in parallel **do**
    $(\mathbf{A}_{k,t}, \mathbf{Y}_k) \leftarrow$ ClientUpdate$(\mathbf{W}^{\mathrm{C}}_{k,t})$
    Forward propagation with $\mathbf{A}_{k,t}$ on $\mathbf{W}^{\mathrm{S}}_t$, compute $\hat{\mathbf{Y}}_k$
    Loss calculation with $\mathbf{Y}_k$ and $\hat{\mathbf{Y}}_k$
    Back-propagation calculate $\triangledown \ell_k(\mathbf{W}^{\mathrm{S}}_t; \mathbf{A}^{\mathrm{S}}_t)$
    Send $d\mathbf{A}_{k,t} := \triangledown \ell_k(\mathbf{A}^{\mathrm{S}}_t; \mathbf{W}^{\mathrm{S}}_t)$ (i.e., gradient of the $\mathbf{A}_{k,t}$) to client k for ClientBackprop$(d\mathbf{A}_{k,t})$
  end
  Server-side model update: $\mathbf{W}^{\mathrm{S}}_{t+1} \leftarrow \mathbf{W}^{\mathrm{S}}_t - \eta \frac{n_k}{n} \sum_{i=1}^{K} \triangledown \ell_i(\mathbf{W}^{\mathrm{S}}_t; \mathbf{A}^{\mathrm{S}}_t)$

/* Runs on Client k */
EnsureClientUpdate$(\mathbf{W}^{\mathbf{C}}_{k,t})$**:**
  Model updates $\mathbf{W}^{\mathrm{C}}_{k,t} \leftarrow$ FedServer$(\mathbf{W}^{\mathrm{C}}_{t-1})$
  Set $\mathbf{A}_{k,t} = \phi$
  for each local epoch e from 1 to E **do**
    for batch $b \in \mathcal{B}$ **do**
      Forward propagation on $\mathbf{W}^{\mathrm{C}}_{k,b,t}$
      Concatenate the activations of its final layer to $\mathbf{A}_{k,t}$
      Concatenate respective true labels to $\mathbf{Y}_k$
    end
  end
  Send $\mathbf{A}_{k,t}$ and $\mathbf{Y}_k$ to the main server

/* Runs on Client k */
EnsureClientBackprop$(d\mathbf{A}_{k,t})$**:**
  for batch $b \in \mathcal{B}$ **do**
    Back-propagation, calculate gradients $\triangledown \ell_k(\mathbf{W}^{\mathrm{C}}_{k,b,t})$
    $\mathbf{W}^{\mathrm{C}}_{k,t} \leftarrow \mathbf{W}^{\mathrm{C}}_{k,t} - \eta \triangledown \ell_k(\mathbf{W}^{\mathrm{C}}_{k,b,t})$
  end
  Send $\mathbf{W}^{\mathrm{C}}_{k,t}$ to the Fed server

/* Runs on Fed Server */
EnsureFedServer executes:
  for each client $k \in S_t$ in parallel **do**
    $\mathbf{W}^{\mathrm{C}}_{k,t} \leftarrow$ ClientBackprop$(d\mathbf{A}_{k,t})$
  end
  Client-side global model updates: $\mathbf{W}^{\mathrm{C}}_{t+1} \leftarrow \sum_{k=1}^{K} \frac{n_k}{n} \mathbf{W}^{\mathrm{C}}_{k,t}$
  Send $\mathbf{W}^{\mathrm{C}}_{t+1}$ to all K clients for ClientUpdate$(\mathbf{W}^{\mathrm{C}}_{k,t})$

Table 3: Total cost analysis of the four DCML approaches

Method	Comms. per client	Total comms.	Total model training time	Total cost
FL	$2\|W\|$	$2K\|W\|$	$t + K\|W\|$	$t + 3K\|W\|$
SL	$(\frac{2p}{K})q + 2\beta\|W\|$	$2pq + 2\beta K\|W\|$	$tK + T(K-1)$	$2pq + 2\beta K\|W\| + tK + T(K-1)$
SFLV1	$(\frac{2p}{K})q + 2\beta\|W\|$	$2pq + 2\beta K\|W\|$	$t + K\|W\|$	$2pq + t + (1 + 2\beta)K\|W\|$
SFLV2	$(\frac{2p}{K})q + 2\beta\|W\|$	$2pq + 2\beta K\|W\|$	$t + \beta K\|W\|$	$2pq + t + 3\beta K\|W\|$

4 Splitfed threat model and privacy

In this work, we consider all clients, the fed server, and the main server of our system model are honest-but-curious adversaries. They perform the tasks as specified but can be curious about the local private data of the clients. The attack scenario considered here is passive, where they only observe the updates and possibly do some calculations to get the information, but they do not maliciously modify their own inputs or parameters for the attack purpose. Besides, the servers and clients are non-colluding with each other. We assume that SFLV1 and

SFLV2 (our approaches) adheres to the standard client-server security model where the clients and servers establish a certain level of trust before starting the network model training. For example, in the health domain, the hospitals (clients) only allow researchers (server) which have a level of trust. Hospitals opt-out if the corresponding platform has malicious clients or servers. Besides, we assume that all communications between the participating entities (e.g., exchange of smashed data and gradients between clients and the main server) are performed in an encrypted form. Privacy in SFL (both versions) is enabled by MTD approach and network split. The latter is discussed in the following section.

4.1 Privacy due to network split

Network split and ML learning enables the clients and the main server maintain privacy by not allowing the server to get the client-side model updates and vice-versa. The server has access only to the smashed data (i.e., activation vectors of the cut layer). A curious server needs to invert all the client-side model parameters, i.e., weight vectors. The possibility to infer the client-side model parameters and raw data is highly unlikely if we allow the fully connected layers with sufficiently large nodes at the client-side ML network [12]. However, for a smaller client-side network, this possibility can be high. This issue can be reduced by modifying the loss function at the client-side [18].

5 Experiment setup

Experiments are carried out on uniformly distributed and horizontally partitioned image datasets among clients. All programs are written in python 3.7.2 using the PyTorch library (PyTorch 1.2.0). For quicker experiments and developments, we use the High-Performance Computing (HPC) platform[6] where we run clients and servers on different computing nodes of the cluster. We request the following resources for one slurm job on HPC: 10GB of RAM, one GPU (Tesla P100-SXM2-16GB), one computing node with at least one task per node. The architecture of the node is x86_64. During the experiments, we investigate the performance by observing the training time (also called latency) w.r.t. global epochs, and the amount of data communication by each client. In our setup, we consider that all participants update the model in each global epoch (i.e., $C = 1$ during training). We choose ML network architectures and datasets based on their performance and their need to include in our studies for proportionate participation. The learning rate for LeNet is maintained at 0.004, and 0.0001 for the remainder network architectures (AlexNet, ResNet and VGG16). We choose the learning rate based on their performance during our initial observations. For example, for LeNet on FMNIST, we observed train and test accuracy of 94.8% and 92.1% with a learning rate of 0.004, whereas 87.8% and 87.3% with a learning rate of 0.0001 in 200 global epochs. We set up a similar computing environment and perform the comparative analysis. We do not conduct hyperparameter tunning or any other model optimization scenarios, as our work is on the privacy-preserving approaches in DCML rather than the optimization of the individual ML network.

5.1 Datasets

We use four public image datasets in our experiments, and these are summarized in Table 4. HAM10000 dataset is a medical dataset, i.e., the Human Against Machine with 10000 training images [19]. It consists of colored images of pigmented skin lesion, and has dermatoscopic images from different populations, acquired and stored by different modalities. Each sample has 600×450 pixel images. HAM10000 has a total of $10,015$ samples with seven cases of important diagnostic categories: Akiec, bcc, bkl, df, mel, nv and vasc. MNIST dataset consists of handwritten digit images of 0 to 9 (i.e., 10 classes). Each image has 28×28 pixels with a pixel value ranges from 0 to 255. It has a total of $60,000$ training and $10,000$ test samples. Fashion MNIST consists of images of ten clothing, including T-shirts, trousers, pullover, dress, and coat. Each sample has 28×28 pixel grayscale images the number of training and test samples equal to the MNIST dataset. CIFAR10 consists of color images of ten objects (classes), including airplane, cat, dog, bird, automobile, horse, and ship. It has $50,000$ training and $10,000$ test samples. Each sample in CIFAR10 has 32×32 pixels. For our experiments, we consider the training and testing sample sizes depicted in Table 4. In our DCML setup, the dataset is randomly, disjointly, and uniformly distributed among clients.

5.2 Model Architecture

We consider four ML model architectures in our experiments. These four architectures fall under Convolutional Neural Network (CNN) and are summarized in Table 5. We restrict our experiments to CNN architectures, and

[6] CSIRO's HPC resource, named Bracewell, is employed. It is built on Dell EMC's PowerEdge platform with partner GPUs for computation and InfiniBand networking.

Table 4: Datasets

Dataset	Training samples	Testing samples	Image size
HAM10000 [19]	9013	1002	600×450
MNIST [20]	$60,000$	$10,000$	28×28
FMNIST [21]	$60,000$	$10,000$	28×28
CIFAR10 [22]	$50,000$	$10,000$	32×32

Table 5: Model Architecture

Architecture	No. of parameters	Layers	Kernel size
LeNet [23]	60 thousands	5	(5×5), (2×2)
AlexNet [2]	60 million	8	(11×11), (5×5), (3×3)
VGG16 [24]	138 million	16	(3×3)
ResNet18 [25]	11.7 million	18	(7×7), (3×3)

further experiments on other architectures such as recurrent neural networks will be investigated in future work. LeNet [23] is a five-layer CNN consisting of convolution, average pooling, Sigmoid or Tanh, and fully connected layers. It uses the 5×5 and 2×2 sized kernels in its layers. The input image dimension is $32 \times 32 \times 1$. AlexNet [2] consists of eight layers of network, including convolution (five layers), pooling (three layers), and fully connected (two) layers. It uses 11×11, 5×5, and 3×3 sized kernels in its layers. The input image dimension is $227 \times 227 \times 3$. VGG16 [24] consists of sixteen layers of network, including convolution (sixteen layers), max pooling, and fully connected layers. It uses 3×3 sized kernels in its layers. The input image dimension is $224 \times 224 \times 3$. ResNet18 [25] consists of eighteen layers of network, including convolution, max pooling, ReLU, and fully connected layers. It uses 7×7 and 3×3 sized kernels in its layers.

For all experiments in SL, SFLV1 and SFLV2, the network layers are split at the following layer: second layer of LeNet (after 2D MaxPool layer), second layer of AlexNet (after 2d MaxPool layer), fourth layer of VGG16 (after 2D MaxPool layer), and third layer (after 2D BatchNormalization layer) of ResNet18.

6 Empirical Results and Discussion

6.1 How do the distributed collaborative machine learning, including splitfedv1 and splitfedv2 perform?

We consider the results under standard learning (centralized learning) as our benchmark. In standard learning, all data are available centrally to a server that performs ML training and testing. Table 6 and 7 summarize our first result, where the observation window is 200 global epochs with one local epoch, batch size of 1024, and five clients for DCML. The tables show the highest accuracy observed at 200 global epochs; thus, it is not necessarily the accuracy at the final global epoch (i.e., 200). Moreover, the accuracy is averaged over all clients in the DCML setup.

Analyzing Table 6 and 7: As presented in the tables, SL and SFL (both versions) performed well under the proposed experimental setup. However, we also observed that among DCML, FL has better learning performance in most cases as the original model is not split while trained among the multiple clients. In all cases except ResNet18 on MNIST, the four approaches failed to achieve the benchmark results. Based on the results in Table 6 and 7, we can observe that SFLV1 and SFLV2 have inherited the characteristics of SL. We noticed that VGG16 on CIFAR10 did not converge in SL, which was the same for both versions of splitfed learning although there was around 66% and 67% of train and test accuracies, respectively, for FL. We assume that this was because of the unavailability of certain other factors such as, hyper-parameters tuning or change in data distribution, which are out of the scope of this paper. Besides, in some cases, the train accuracy was less than the test accuracy. This may be due to the use of dropouts, the less diversity in test data, and the consideration of the highest accuracy within the observation window (i.e., 200 global epochs).

In the following, we present and discuss the performance of the ResNet18 on HAM10000 dataset for standard configuration, FL, SL, SFLV1, and SFLV2 under similar settings. The training and testing performances of the remaining architectures and datasets are provided in Appendix A.3.

Table 6: Training Results

Dataset	Architecture	Normal	Federated	Split	Splitfedv1	Splitfedv2
HAM10000	ResNet18	99.8%	92.2%	99.5%	90.2%	99.3%
HAM10000	AlexNet	98.8%	74.2 %	70.3%	69%	72.1%
FMNIST	LeNet	95.1%	92.5 %	90.6%	89%	89.6%
FMNIST	AlexNet	97.2%	90.6 %	83.9%	84.9%	79%
CIFAR10	LeNet	78.7%	70.5 %	62.6%	61.3%	62%
MNIST	AlexNet	99.7%	98.8%	93.7%	95.7%	89.8%
MNIST	ResNet18	99.9%	99.9%	99.9%	99.8%	99.9%

Table 7: Test Results

Dataset	Architecture	Normal	Federated	Split	Splitfedv1	Splitfedv2
HAM10000	ResNet18	79.3%	77.5%	79.1%	79%	79.2%
HAM10000	AlexNet	80.1%	75 %	73.8%	70.5%	74.9%
FMNIST	LeNet	92.7%	91.9 %	90.4%	89.6%	90.4%
FMNIST	AlexNet	90.5%	89.7%	84.7%	86%	81%
CIFAR10	LeNet	72.1%	69.4 %	62.7%	62.6%	63.8%
MNIST	AlexNet	98.8%	98.7 %	95.1%	96.9%	92%
MNIST	ResNet18	99.3%	99.2 %	99.2%	99%	99.2%

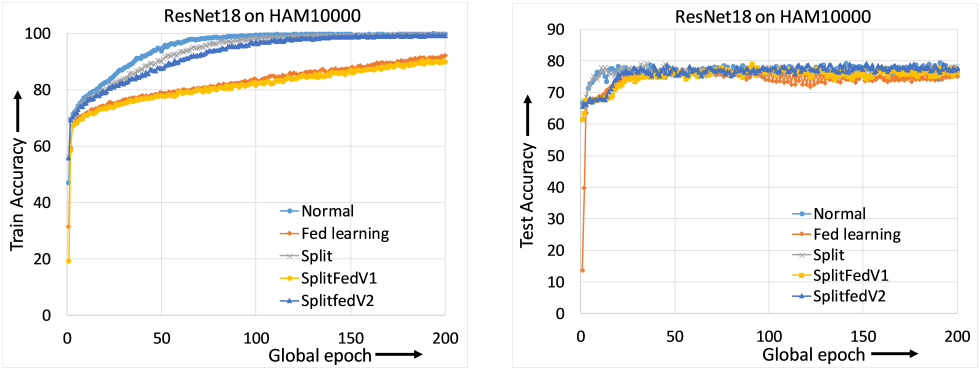

(a) (b)

Fig. 3: (a) Training, and (b) test convergence of ResNet18 on HAM10000 under various learning with five clients.

Analyzing Fig. 3: For ResNet18 on HAM10000, the convergence during training for SFLV1 and FL was close to each other but slower than SFLV2 and SL. The train accuracy reached to around 90% for them, whereas others got 99% in the observation window of 200 global epochs. However, the test accuracy convergence was almost the same for all learning approaches, and they reached to around 76% in the observation window of 200 global epochs. Based on the observation, the performances of SFLV1 and SFLV2 were similar for ResNet18 on HAM10000. However, SFLV1 and SFLV2 struggled to converge if SL failed to converge, as shown in Fig. 8 for the case of VGG16 on CIFAR10.

In some datasets and architecture, the train accuracy of the model was still improving and showing better performance at higher global epochs than 200. For example, going from 200 epochs to 400 epochs, we noticed an accuracy increment from 84.7% to 86.9% for FL with LeNet on FMNIST with 100 users. However, we limited our observation window to 200 global epochs as some network architecture such as AlexNet on HAM10000 in FL was taking an extensive amount of training time on the HPC (a shared resource).

6.2 Effect of number of users on the performance

In this section, we present the analysis of the effect of the number of users for ResNet18 on HAM10000. Refer to Appendix A.4 for the results of LeNet on FMNIST and AlexNet on HAM10000. For ResNet18 on HAM10000, we observed that up to 100 clients (clients ranging from 5 to 100), the train and test curves for all numbers of clients followed a similar pattern in each plot. Moreover, they achieved a similar level of accuracy within each of our DCMLs. We got comparative test accuracies of 74% (federated), 77% (split), 75% (SFLV1), and 77% (SFLV2) at

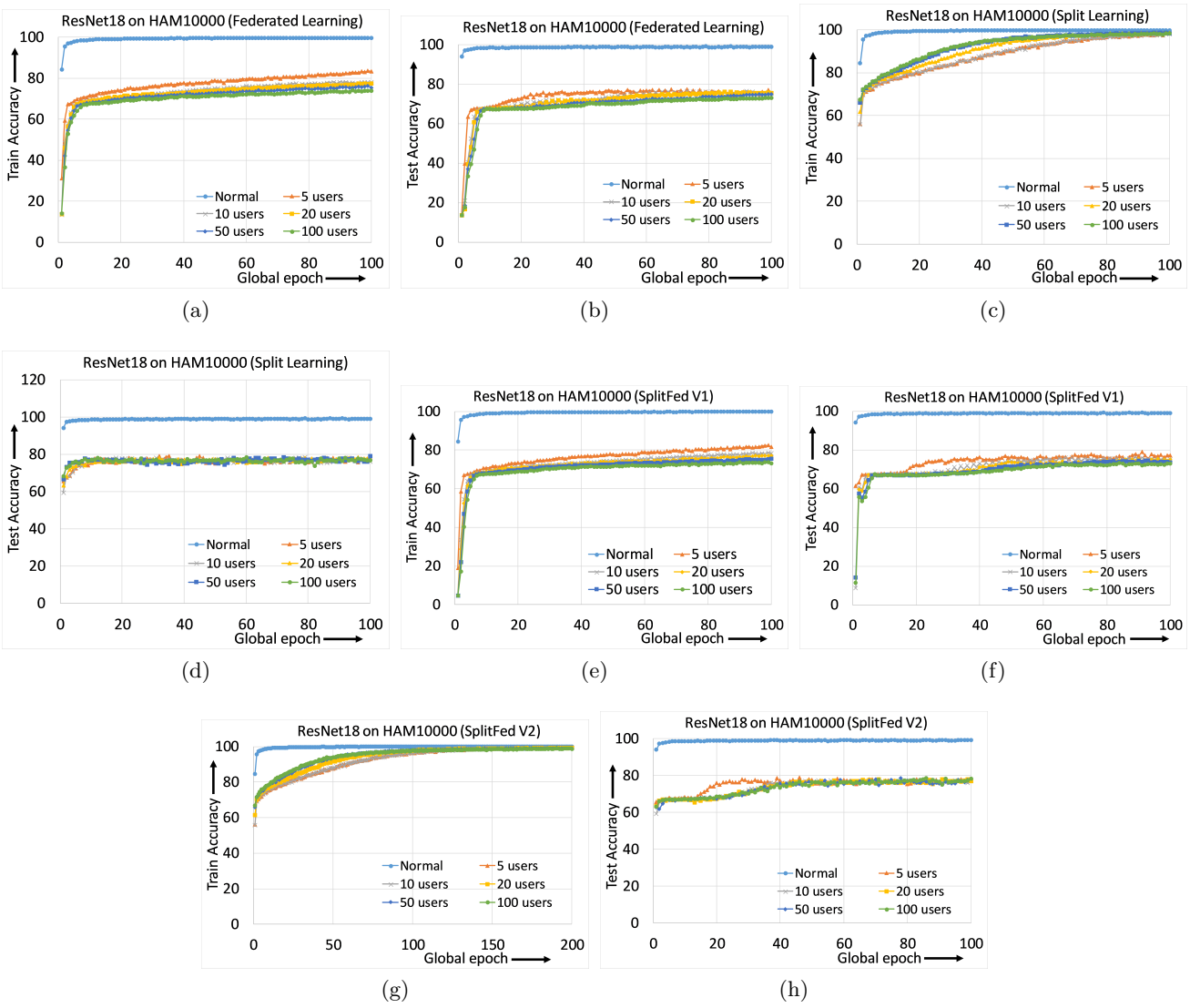

Fig. 4: Training and test convergence of ResNet18 on HAM10000 with various number of clients.

100 global epochs. While training, only SL and SFLV2 achieved the accuracy of the standard training at around 100 global epochs. In contrast, FL and SFLV1 could not achieve this result even at 200 global epochs. The experimental results for clients ranging from five to hundred showed a negligible effect on the performance due to the increase in the number of clients in FL, SL, SFLV1 and SFLV2. However, there was a significant gap between standard (centralized) learning and DCML (refer to Fig. 4). This was not the case in general. For LeNet on FMNIST with a fewer number of clients, the performances were close to the standard case in FL and SL (refer to Fig. 9). Moreover, for SL with AlexNet on HAM10000, the performance degraded and even failed to converge with the increase in the number of clients, and we saw a similar effect on the SFLV2 (refer to Fig. 10). Overall, the convergence of the learning and performance slowed down (sometimes failed to progress) with the increase in the number of clients in our DCML techniques due to the resource limitations and other constraints of the experimental setup.

6.3 Communication measurement

The amount of data uploaded and downloaded by a client indicates the operability of a DCML approach in a resource constrained environment. High data communication slows down the ML training and testing process, and the clients need to have sufficient resources to handle the high communication cost. In this regard, we measure the amount of data communication in our experiments and present the relative performance of the four DCML techniques. To make the experimental setup normalized for different number of clients, we run our program under the following configurations: The main server's and fed server's programs run in two different HPC nodes, and

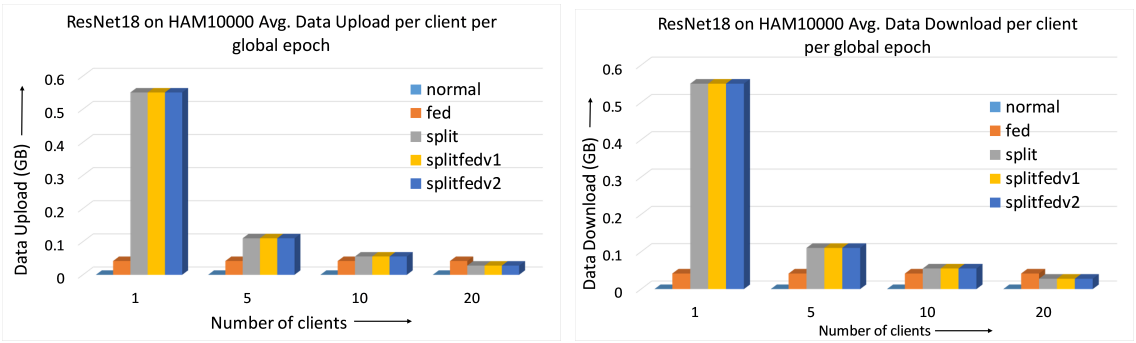

(a) (b)

Fig. 5: (a) Data upload, and (b) data download for ResNet18 on HAM10000 with various number of clients.

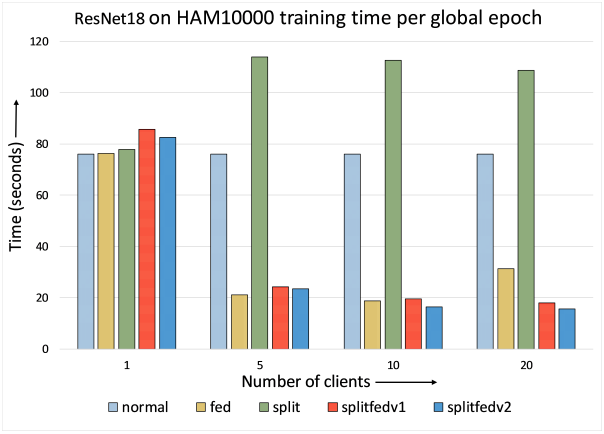

Fig. 6: Time measurement for ResNet18 on HAM10000 with various number of clients.

clients' programs run in five separate nodes (except for experiment with one client). Each client HPC node runs one, two, and four clients (client-side programs) for five, ten, and twenty client cases, respectively. We record the total communication for the observation window of 11 global epochs with one local epoch and a batch size of 256. Then, the results were averaged over all global epochs and clients to obtain the communication cost per client per global epoch.

During the experiments, we observed the same amount of data communication for SL, SFLV1, and SFLV2. For example, refer to Fig. 5 and 7. This showed that SFLV1 and SFLV2 provided the same communication efficiency of SL. As the number of clients increased, the amount of data communication (which was averaged over clients) per global epoch decreased for SL, SFLV1 and SFLV2. This was because of the following two reasons: (1) SL and both versions of SFL were communicating smashed data rather than (model) weights. Thus, the amount of communication was the function of the data samples. (2) The overall dataset was uniformly distributed among clients, so the dataset size per client decreased with the increase in the number of clients. On the other hand, this effect was not applicable to FL, which had the same level of data communication in all cases. This was because, in FL, for a given network architecture, each client sent the locally trained network to the server and received the global network independent of the sample size.

In a recent work, it was shown that SL is communication efficient than FL with the increase in the number of clients or model size. In contrast, FL is preferred if the amount of data samples is increased by keeping the number of clients or model size low [26,27]. Our results in Fig. 5 and 7 complement this result for SL and FL.

6.4 Time measurement

To show the time efficiency of splitfed learning (both versions) compared to SL, we analyze the training time taken for one global epoch. Considering Section 3, Algorithms 2 and 3, it is not difficult to see the following: (1) For SL, the total training time for one global epoch depends on the product of *the number of clients* and *the time to process one global epoch by the clients and the server*, and (2) in SFLV1, there are no such product terms while calculating

the time because the server can be a supercomputing resource and processes all clients in parallel. Consequently, SFLV1 is faster than SL for multiple clients. Besides, this also shows that the training time measurement depends not only on the implementation but also on the algorithm. For our experiments in SFLV1, we implemented a multithreaded python program for the main server. By using the same experimental setup (which was used to measure the communication cost), we ran each experiment for eleven global epochs and recorded the time for each global epoch. Unlike in the communication measurement setup, the training time was averaged by considering the time from the second global epoch onward for all clients after running each experiment for 10 times. The time for the first global epoch was excluded because it included the time taken by clients to connect to the server, i.e., initial connection overhead (in our setup, all clients got connected to the server at first and kept the connection during the experiment). We ran each experiment for ten times - different HPC slurm jobs in each instance - to exclude the effects of the change in the computing environment in each run.

Based on our observations on ResNet18 on HAM10000 and AlexNet on MNIST, time statistics for the cases with multiple clients indicated that SFLV1 and SFLV2 were significantly faster - around five times - than SL. It had a similar or even better speed than FL (refer to Fig. 6 and 8). For the single client case, all other DCML approaches spent similar time; SFLV1 and SFLV2 spent slightly higher than the other.

7 Limitations and future works

In this study, we have analyzed the performance of FL, SL, SFLV1, and SFLV2 based on their privacy-preserving features, model accuracy, communication, and computation costs. The comparative performance analysis of these privacy-preserving distributed ML approaches with the integration of DP [6,28] and HE [5] is remained as future work. Moreover, DP provides provable privacy, whereas fully HE provides guaranteed privacy. However, they have a negative effect on model performance and computational overhead, respectively.

8 Conclusion

By bringing federated learning (FL) and split learning (SL) together, we proposed a novel distributed machine learning approach, named splitfed, that offered a higher level of privacy than FL due to network splitting, faster than SL due to parallel processing across clients. Results showed that splitfed provides similar performance in terms of model accuracy compared to SL. Thus, as being a hybrid approach, it is suitable for ML with low-computing resources (enabled by network split), fast training (enabled by handling clients in parallel), and analytic over private and sensitive data. Our empirical results for ResNet18 on HAM10000 and AlexNet on MNIST showed that the two versions of splitfed learning (presented in this paper) were significantly faster than SL for multiple clients. Moreover, their speed was similar or even better than FL in certain cases, and they had the same communication efficiency of SL and improved its efficiency than FL with the increase in the number of clients.

References

1. Guosheng Hu, Xiaojiang Peng, Yongxin Yang, Timothy M. Hospedales, and Jakob Verbeek. Frankenstein: Learning deep face representations using small data. *IEEE Trans. Image Processing*, 27(1):293–303, 2018.
2. Alex Krizhevsky, Ilya Sutskever, and Geoffrey E. Hinton. Imagenet classification with deep convolutional neural networks. In *Proc. NIPS'12 - Vol. 1*, pages 1097–1105, USA, 2012.
3. J. Guinney and J. Saez-Rodriguez. Alternative models for sharing confidential biomedical data. *Nature BioTech.*, 36(5):391–392, May 2018.
4. EU. Regulation (eu) 2016/679 general data protection regulation. *Official Journal of the European Union*, May 2016.
5. Craig Gentry. *A fully homomorphic encryption scheme*. PhD thesis, Stanford University, Stanford, California, Sept. 2009.
6. Cynthia Dwork and Aaron Roth. The algorithmic foundations of differential privacy. *Foundations and Trends in Theoretical Computer Science*, 9(3-4):211–407, 2014.
7. Andrew C. Yao. Protocols for secure computations. In *Proc. SFCS '82*, pages 160–164. IEEE Computer Society, 1982.
8. Le Trieu Phong, Yoshinori Aono, Takuya Hayashi, Lihua Wang, and Shiho Moriai. Privacy-preserving deep learning via additively homomorphic encryption. *IEEE Trans. Info. Forensics and Security*, 13(5):1333–1345, 2018.
9. Keith Bonawitz, Vladimir Ivanov, Ben Kreuter, Antonio Marcedone, H. Brendan McMahan, Sarvar Patel, Daniel Ramage, Aaron Segal, and Karn Seth. Practical secure aggregation for privacy-preserving machine learning. In *Proc. CCS '17*, pages 1175–1191. ACM, 2017.
10. Jakub Konecný, Brendan McMahan, and Daniel Ramage. Federated optimization: Distributed optimization beyond the datacenter. *CoRR*, abs/1511.03575, 2015.

11. Brendan McMahan, Eider Moore, Daniel Ramage, Seth Hampson, and Blaise Agüera y Arcas. Communication-efficient learning of deep networks from decentralized data. In *Proc. AISTATS*, pages 1273–1282, 2017.
12. Otkrist Gupta and Ramesh Raskar. Distributed learning of deep neural network over multiple agents. *J. Network and Computer Applications*, 116:1–8, 2018.
13. Jianmin Chen, Rajat Monga, Samy Bengio, and Rafal Jzefowicz. Revisiting distributed synchronous sgd. In *2016 Proc. of ICLR workshop track*, 2016.
14. Jeffrey Dean, Greg Corrado, Rajat Monga, Kai Chen, Matthieu Devin, Quoc V. Le, Mark Z. Mao, Marc'Aurelio Ranzato, Andrew W. Senior, Paul A. Tucker, Ke Yang, and Andrew Y. Ng. Large scale distributed deep networks. In *NIPS*, pages 1232–1240, 2012.
15. Keith Bonawitz, Hubert Eichner, Wolfgang Grieskamp, Dzmitry Huba, Alex Ingerman, Vladimir Ivanov, Chloé Kiddon, Jakub Konecný, Stefano Mazzocchi, H. Brendan McMahan, Timon Van Overveldt, David Petrou, Daniel Ramage, and Jason Roselander. Towards federated learning at scale: System design. 2019.
16. Praneeth Vepakomma, Otkrist Gupta, Tristan Swedish, and Ramesh Raskar. Split learning for health: Distributed deep learning without sharing raw patient data. 2018.
17. Sharif Abuadbba, Kyuyeon Kim, Minki Kim, Chandra Thapa, Seyit A. Camtepe, Yansong Gao, Hyoungshick Kim, and Surya Nepal. Can we use split learning on 1d cnn models for privacy preserving training?, 2020.
18. Praneeth Vepakomma, Otkrist Gupta, Abhimanyu Dubey, and Ramesh Raskar. Reducing leakage in distributed deep learning for sensitive health data. In *Proc. ICLR*, 2019.
19. Philipp Tschandl. The HAM10000 dataset, a large collection of multi-source dermatoscopic images of common pigmented skin lesions, 2018.
20. Y. Lecun, L. Bottou, Y. Bengio, and P. Haffner. Gradient-based learning applied to document recognition. *Proc. of the IEEE*, 86(11):2278–2324, Nov 1998.
21. Han Xiao, Kashif Rasul, and Roland Vollgraf. Fashion-mnist: a novel image dataset for benchmarking machine learning algorithms. *CoRR*, abs/1708.07747, 2017.
22. Alex Krizhevsky, Vinod Nair, and Geoffrey Hinton. Cifar-10 (canadian institute for advanced research).
23. Y. Lecun, L. Bottou, Y. Bengio, and P. Haffner. Gradient-based learning applied to document recognition. *Proc. of the IEEE*, 86(11):2278–2324, Nov 1998.
24. Karen Simonyan and Andrew Zisserman. Very deep convolutional networks for large-scale image recognition. In *Proc. 3rd ICLR*, 2015.
25. K. He, X. Zhang, S. Ren, and J. Sun. Deep residual learning for image recognition. In *2016 IEEE CVPR*, pages 770–778, June 2016.
26. Abhishek Singh, Praneeth Vepakomma, Otkrist Gupta, and Ramesh Raskar. Detailed comparison of communication efficiency of split learning and federated learning, 2019.
27. Yansong Gao, Minki Kim, Sharif Abuadbba, Yeonjae Kim, Chandra Thapa, Kyuyeon Kim, Seyit A. Camtepe, Hyoungshick Kim, and Surya Nepal. End-to-end evaluation of federated learning and split learning for internet of things, 2020.
28. Pathum Chamikara Mahawaga Arachchige, Peter Bertok, Ibrahim Khalil, Dongxi Liu, Seyit Camtepe, and Mohammed Atiquzzaman. Local differential privacy for deep learning. *IEEE Internet of Things Journal*, 2019.
29. William Gropp, William D Gropp, Ewing Lusk, Argonne Distinguished Fellow Emeritus Ewing Lusk, and Anthony Skjellum. *Using MPI: portable parallel programming with the message-passing interface*, volume 1. MIT press, 1999.
30. Jason Sanders and Edward Kandrot. *CUDA by example: an introduction to general-purpose GPU programming, portable documents*. Addison-Wesley Professional, 2010.
31. Antonio Gulli and Sujit Pal. *Deep learning with Keras*. Packt Publishing Ltd, 2017.
32. Adam Paszke, Sam Gross, Francisco Massa, Adam Lerer, James Bradbury, Gregory Chanan, Trevor Killeen, Zeming Lin, Natalia Gimelshein, Luca Antiga, et al. Pytorch: An imperative style, high-performance deep learning library. In *Advances in Neural Information Processing Systems*, pages 8024–8035, 2019.
33. Milind Bhandarkar. Mapreduce programming with apache hadoop. In *2010 IEEE International Symposium on Parallel & Distributed Processing (IPDPS)*, pages 1–1. IEEE, 2010.
34. James G Shanahan and Laing Dai. Large scale distributed data science using apache spark. In *Proceedings of the 21th ACM SIGKDD international conference on knowledge discovery and data mining*, pages 2323–2324, 2015.
35. Martín Abadi, Paul Barham, Jianmin Chen, Zhifeng Chen, Andy Davis, Jeffrey Dean, Matthieu Devin, Sanjay Ghemawat, Geoffrey Irving, Michael Isard, et al. Tensorflow: A system for large-scale machine learning. In *12th {USENIX} Symposium on Operating Systems Design and Implementation ({OSDI} 16)*, pages 265–283, 2016.
36. Elias De Coninck, Steven Bohez, Sam Leroux, Tim Verbelen, Bert Vankeirsbilck, Pieter Simoens, and Bart Dhoedt. Dianne: a modular framework for designing, training and deploying deep neural networks on heterogeneous distributed infrastructure. *Journal of Systems and Software*, 141:52–65, 2018.
37. Zvika Brakerski and Vinod Vaikuntanathan. Efficient fully homomorphic encryption from (standard) lwe. *SIAM Journal on Computing*, 43(2):831–871, 2014.
38. Pathum Chamikara Mahawaga Arachchige, Peter Bertok, Ibrahim Khalil, Dongxi Liu, Seyit Camtepe, and Mohammed Atiquzzaman. A trustworthy privacy preserving framework for machine learning in industrial iot systems. *IEEE Transactions on Industrial Informatics*, 2020.
39. Josep Domingo-Ferrer, Oriol Farras, Jordi Ribes-González, and David Sánchez. Privacy-preserving cloud computing on sensitive data: A survey of methods, products and challenges. *Computer Communications*, 140:38–60, 2019.

40. Keith Bonawitz, Hubert Eichner, Wolfgang Grieskamp, Dzmitry Huba, Alex Ingerman, Vladimir Ivanov, Chloe Kiddon, Jakub Konecny, Stefano Mazzocchi, H Brendan McMahan, et al. Towards federated learning at scale: System design. *arXiv preprint arXiv:1902.01046*, 2019.

41. Praneeth Vepakomma, Otkrist Gupta, Tristan Swedish, and Ramesh Raskar. Split learning for health: Distributed deep learning without sharing raw patient data. *arXiv preprint arXiv:1812.00564*, 2018.

A Supplemental Figures

A.1 Communication measurement

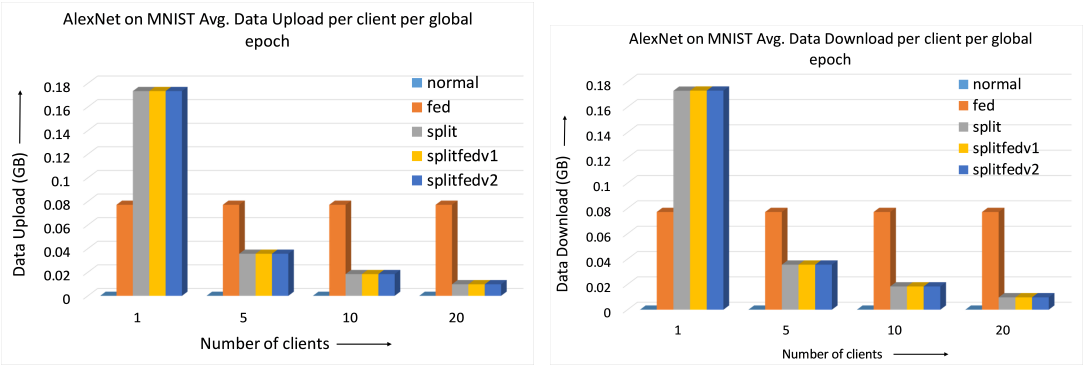

(a) (b)

Fig. 7: (a) Data upload, and (b) data download for AlexNet on MNIST with various number of clients.

A.2 Training time measurement

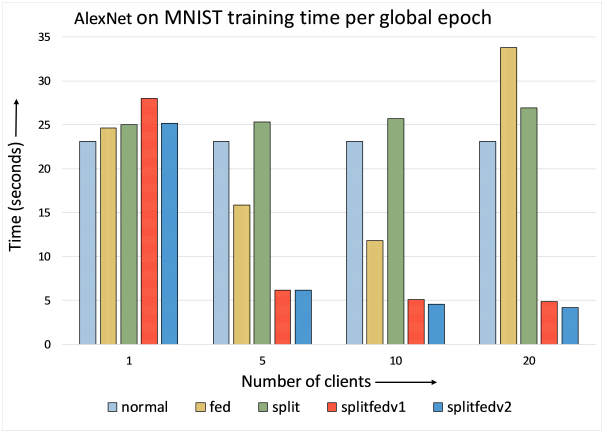

Fig. 8: Time measurement for AlexNet on MNIST with various number of clients.

A.3 Learning and performance curves

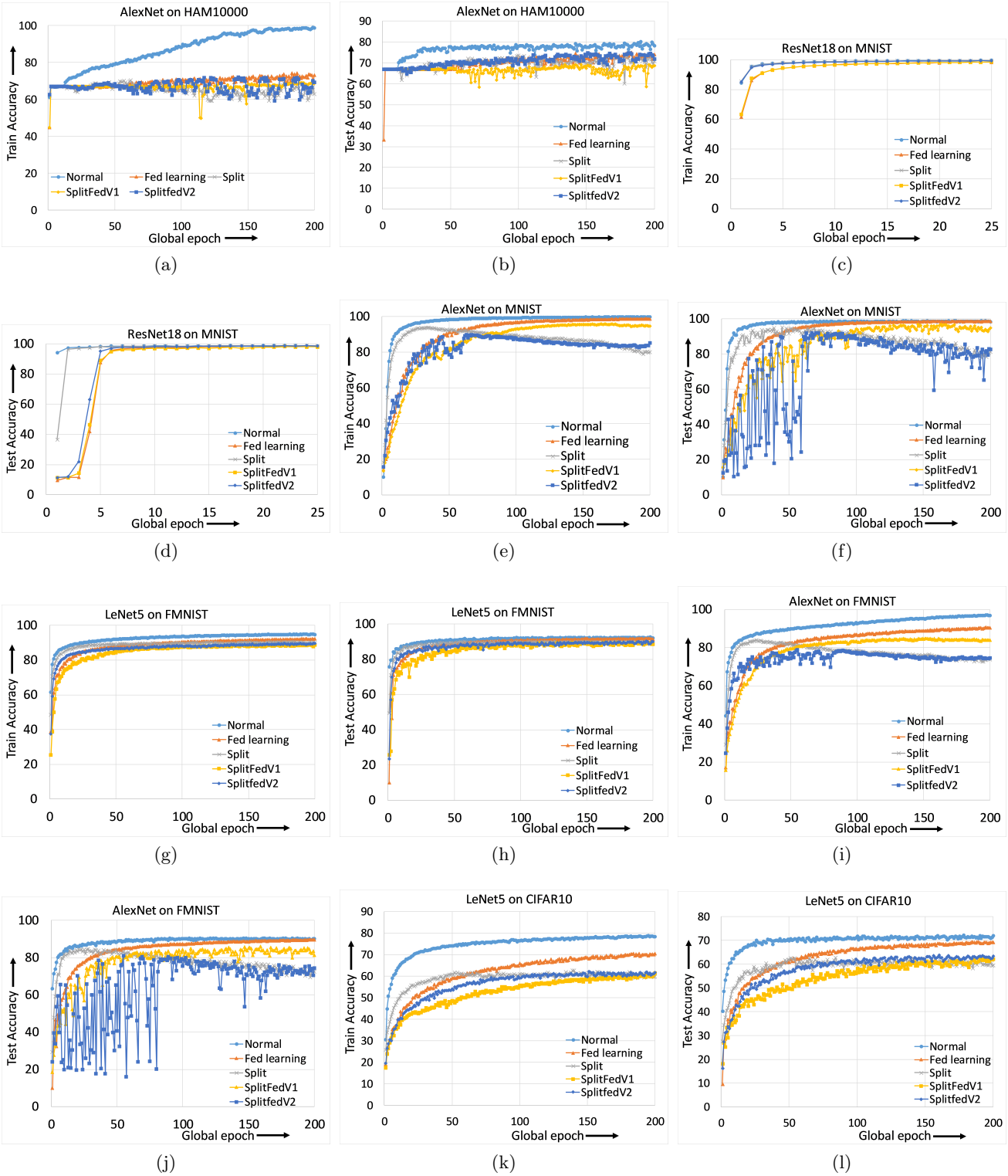

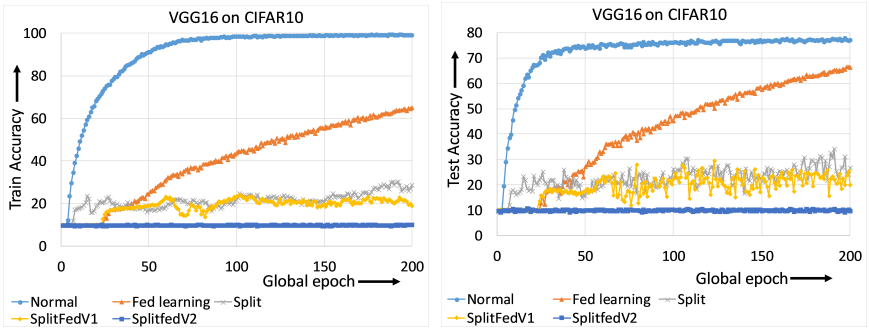

(m) (n)

Fig. 8: Training and test convergence with five clients under various DCML approaches, architectures and datasets.

A.4 Effects of number of users on the performance

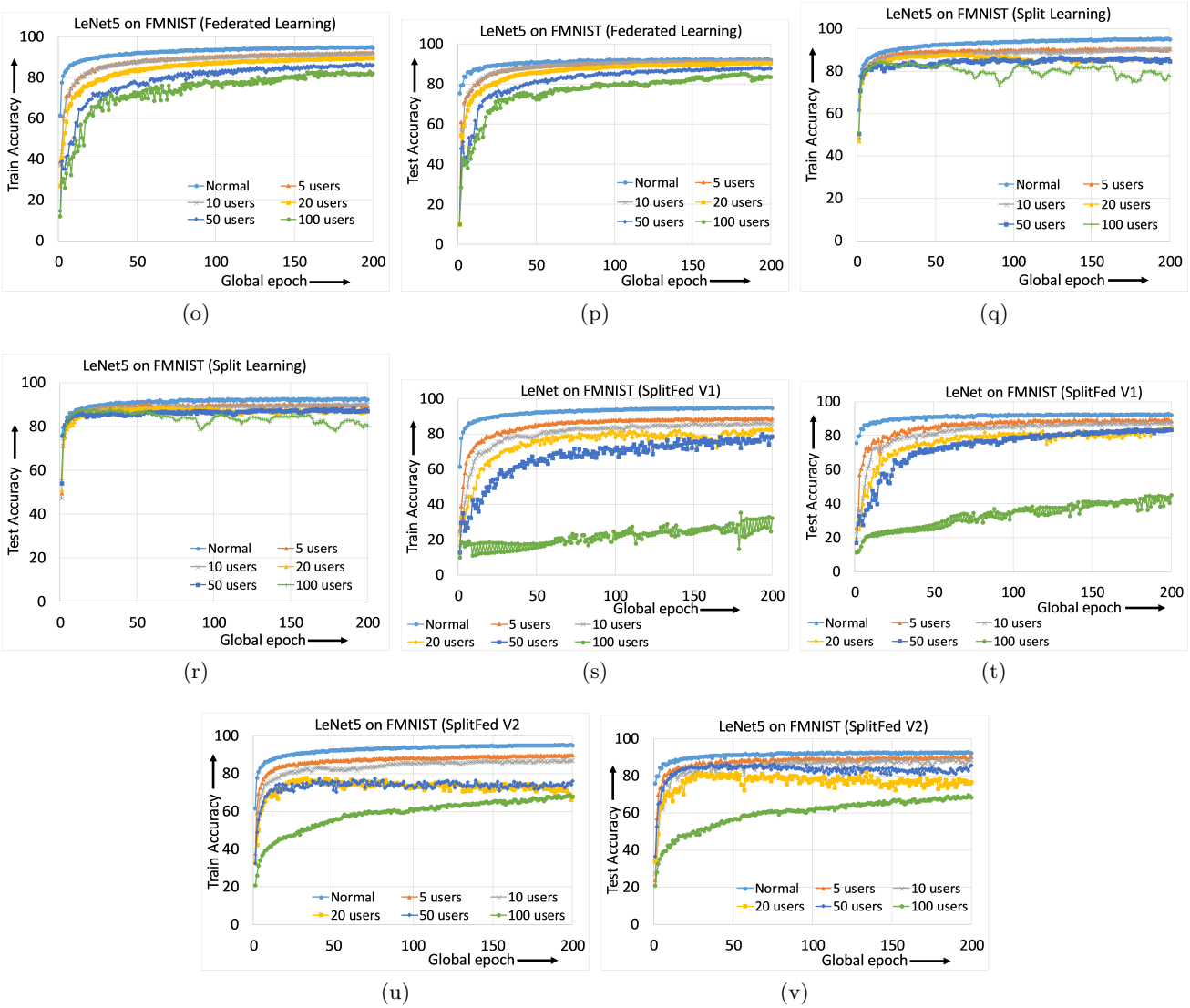

(o) (p) (q)

(r) (s) (t)

(u) (v)

Fig. 9: Effects of number of users for LeNet on FMNIST: Training and test convergence with various number of clients and DCML approaches.

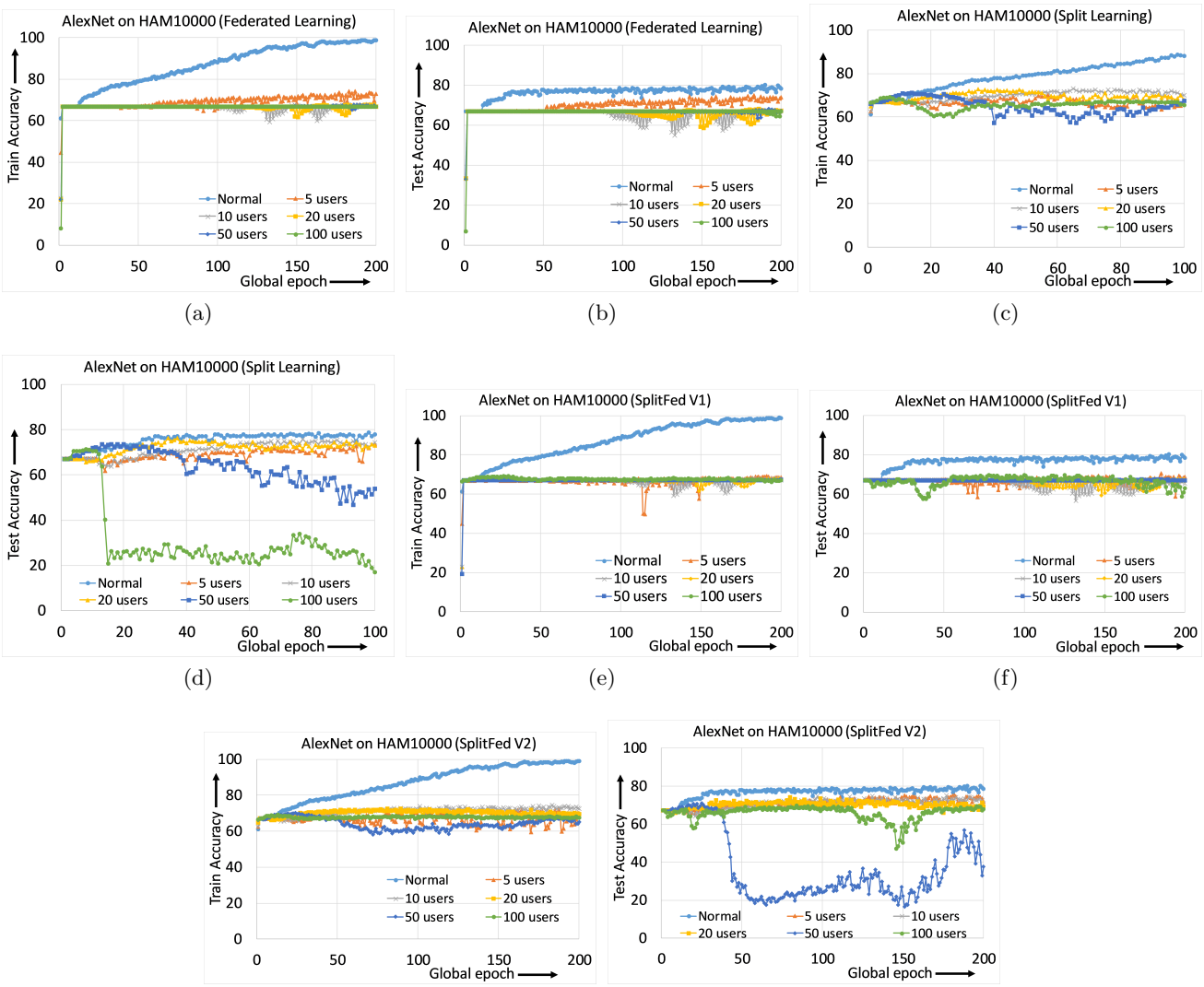

Fig. 10: Effects of number of users for AlexNet on HAM10000: Training and test convergence with various number of clients and DCML approaches.